

## MODELING AND IDENTIFICATION OF A PNEUMATIC MUSCLE ACTUATOR SYSTEM CONTROLLED BY AN ON/OFF SOLENOID VALVE

**V. Jouppila**

Department of Mechanics and Design  
Tampere University of Technology  
33101 Tampere, Finland  
ville.jouppila@tut.fi

**S. A. Gadsden**

Department of Mechanical Engineering  
McMaster University  
Hamilton, Ontario, Canada L8S 4L7  
gadsdesa@mcmaster.ca

**A. Ellman**

Dept. of Mechanics and Design  
Tampere University of  
Technology  
33101 Tampere, Finland  
asko.ellman@tut.fi

### ABSTRACT

Pneumatic actuators offer desirable properties for many applications, such as compactness, low costs, high power-to-weight ratios, reliability, and simplicity. However, due to many nonlinearities (air compressibility, friction, air flow through valve), accurate position and force control of pneumatic actuators is extremely difficult and expensive to achieve. There is a growing interest in PWM-controlled pneumatic systems using low cost on/off solenoid valves instead of servo valves in order to develop less expensive pneumatic servo systems. In addition, a new type of pneumatic McKibben muscle actuator possesses significant advantages like a very high force/weight and force/volume performance, quick response, and wide operational ranges in a variety of environments.

In this paper, a high speed on/off valve is applied to control a pneumatic McKibben muscle actuator system. However, the complex nonlinear dynamics of the actuator in addition to those already mentioned make the modeling and accurate control of the pneumatic system a difficult challenge. As a result, the designed model is nonlinear and may still contain unknown parameters that require identification in order to obtain reasonable dynamical matching with the real system. Furthermore, the discontinuous switching nature of the on/off valve causes transients in the system, making the analytic modeling of the system even more complex.

The objective of this research is to develop an analytical model of the system which includes the nonlinearities of the system, and the transformation of the discontinuities into a continuous form. The use

of analytical models enables the implementation of conventional analytical control approaches, such as sliding mode control, and provides a tool for the analysis of stability and robustness. In this paper, the modeling process is applied to a one degree of freedom pneumatic system for which the analytical nonlinear system model is developed by a combination of physical and empirical methods. An extensive set of experimental tests are performed to characterize the dynamics of the overall system. A non-analytic and analytic model of the system are developed and validated by a comparison of the simulated results with the experimental implementation of the system.

### KEYWORDS

McKibben muscle actuator, on/off solenoid valve, modeling, PWM control

### INTRODUCTION

Pneumatic actuators are commonly avoided for advanced applications due to problems with control caused by the compressibility of air and other nonlinear effects. Pneumatic control systems are mainly used in simple industrial applications with limited requirements for accurate control of motion and force. However, high power-to-weight ratios, compactness, ease of maintenance, and the safety of pneumatic actuators, offer desirable features for many industrial designs. The pneumatic McKibben muscle actuator is a new type of actuator that offers a high force-to-weight ratio and is able to operate in a wide range of environments. The compressibility of air, the nonlinear air flow characteristics through the valves,

friction and the nonlinear characteristics of the McKibben muscle actuator result in a complex and difficult system to model and control.

In the theoretical analysis of pneumatic systems, a combination of thermodynamics, fluid dynamics and the dynamics of the motion is required. The mathematical analysis requires the consideration of the mass flow rates through the valve, the determination of the pressure, volume and temperature of the air in the actuator, and the determination of the dynamics of the load. Furthermore, identification techniques, although usually based on linear methods, can be used for finding the mathematical model of the pneumatic system. An accurate model of the actuator is an important condition for both control design and for optimizing its operation.

In recent years, a considerable amount of research has been performed to develop inexpensive servo-pneumatic systems using on/off solenoid valves with a pulse-width modulation (PWM) technique. In a PWM-controlled system, the power is delivered to the actuator in discrete packets of fluid mass, as the valve is either completely on or off. If the switching frequency of the valve is significantly higher than the system dynamics, the system will act as a low-pass filter responding similarly as to a continuous mass flow input. However, due to the discontinuous switching, the development of an analytical dynamic model of the system is rather difficult, and often prevents the direct use of analytical control designs.

Although previous work has shown the potential of PWM-controlled pneumatics, they have suffered due to the lack of an analytical approach for analyzing the system [1–4]. However, some effort has been made in the area of analytical modeling of such systems [5–7]. A state space averaging approach was presented in [8] for modeling a pulse-width modulation (PWM) based on pneumatic systems. It provided the analytic method necessary to remove the discontinuities associated with switching and resulted in a model suitable to standard nonlinear control design techniques. In [9] a methodology for deriving a nonlinear dynamic model for a pneumatic servo system was presented. The model includes cylinder dynamics, payload motion, friction, and valve characteristics. Experimental results demonstrating the ability of the model to predict the measured position and cylinder chamber pressure were included. In one article, the nonlinearities of the system were handled by proposing a switching controller based on the reduced order nonlinear model of the system [10]. Another notable paper introduced an experimentally developed discrete-time model of a PWM-controlled pneumatic servo system, for which a controller was developed based on discrete-time control methods [11]. Another strategy used a linear state-space averaged model and a linear robust controller based on a loop shaping approach [12]. This approach was later followed by a nonlinear averaged model and a sliding mode controller design [13, 14]. A linearization approach was subsequently used in an attempt to remove the need for complicated nonlinear controllers [15].

The objective of this research is to develop an analytical model of the pneumatic system which includes the nonlinearities of the system, and the transformation of the discontinuities into a continuous form. The use of analytical models enables the implementation of conventional analytical control approaches, such as sliding mode control, and provides a tool for the analysis of stability and robustness. In this paper, the modeling process is

applied to a one degree of freedom pneumatic system where a McKibben muscle actuator mechanism is controlled by a single high-speed solenoid valve. A non-analytical and analytical mass flow rate model through the valve are developed and combined with the nonlinear model of the actuator and the mechanism. An extensive set of experimental tests are performed to characterize the dynamics of the overall system. The models are validated by a comparison of the simulated results with the experimental implementation of the system. Finally, a traditional PI-controller is tuned with the help of a mathematical model, and is implemented in the real system.

## SYSTEM MODELING

### System Setup and Structure

The system hardware is illustrated schematically in Fig. 1. The Festo fluidic muscle (MAS10-300 mm) is hanging vertically, actuating (lifting) the attached payload. The supply pressure (0.65 MPa abs.) for the system is provided by the proportional pressure regulator (Festo VPPM-6L-L1-G18-0L6H-V1N). A single 3/2 high speed on/off solenoid valve (Festo MHE2-1/8-MS1H-3/2G-M7) is controlled to actuate the muscle actuator and the payload. The solenoid is driven by pulsed valve control signal generated in DSpace and Matlab environment. An electronic amplifier is used to provide sufficient power to actuate the valve. A pressure sensor (Festo SDE1-D6-G2-H18-C-PU-M8) provides a feedback signal for the controller. The displacement of the actuator and payload is measured by an electrical potentiometer. Flow restrictors shown between the actuator and valve are optional and can be used to reduce excessive pressure chattering, if necessary. The tubing between the valve and the actuator is kept short as possible, and thus can be neglected in the overall model.

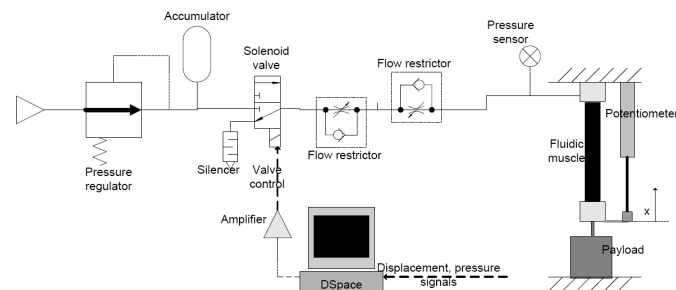


Fig. 1. System setup

### McKibben Muscle Actuator model

The McKibben muscle is an actuator that consists of a rubber tube with a non-extensible fiber surrounding [16]. This physical configuration causes the muscle to have variable-stiffness spring-like characteristics, nonlinear passive elasticity, physical flexibility, and very lightweight compared to other types of actuators [17]. The only commercially available muscle actuator (MAS) by Festo differs slightly from the general McKibben type muscle. The fiber of the fluidic muscle is knit into the tube, offering easy assembly and improved hysteretic behavior and linearity compared to conventional designs [18].

During pressurization of the muscle with air, the muscle widens in diameter and shortens in length. The maximum force is obtained at the beginning of the contraction and decreases with increasing contraction [19]. The actuator is unidirectional and its maximum contraction without load is typically 20% to 25%. The nominal force-to-contraction at different pressure levels is nonlinear, and adds to the difficulty of effectively modeling the muscle actuator. As with all actuation systems, effective application of pneumatic muscle actuators relies on being able to accurately model and predict the forces that will be generated under any operating conditions. In general, the properties of the muscle actuator depend on the geometric parameters shown in Fig. 2.

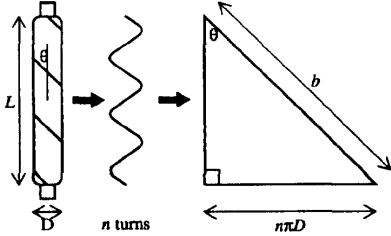


Fig. 2. Geometric model of McKibben actuator [17]

From the geometry of the muscle, the overall length of the actuator and the diameter are given by the following two equations:

$$L = b_s \cos \theta \quad (1)$$

$$D = \frac{b_s \sin \theta}{n_s \pi} \quad (2)$$

Where  $b_s$  is the length of one braid strand, considered to be inextensible, and  $n_s$  is the number of times a strand encircles the muscle's circumference from end-cap to end-cap. Assuming an ideal cylindrical shape, the enclosed volume is defined as follows:

$$V = \frac{b_s^3}{4\pi n_s^2} \cos \theta \sin^2 \theta \quad (3)$$

From the principle of virtual work and the conservation of energy, and assuming quasi-static and lossless conditions, the force required to deform the membrane can be expressed by:

$$F = -p \frac{dV}{dL} \quad (4)$$

Substitution of equation (3) into (4) leads to the force generation equation, first proposed in [19]:

$$F = \frac{\pi D_0^2 p}{4} (3 \cos^2 \theta - 1) \quad (5)$$

Where  $F$  is the contractile muscle force,  $D_0$  is the diameter of the actuator at the braid angle of  $90^\circ$  (theoretical maximum), and  $p$  is the muscle pressure. An improved force equation takes the form [20, 21]:

$$F = (\pi r_0^2) p [a(1 - \varepsilon)^2 - b] \quad (6)$$

$$a = \frac{3}{\tan^2 \theta_0} \quad b = \frac{1}{\sin^2 \theta_0} \quad \varepsilon = \frac{L_0 - L}{L_0}$$

Where  $r_0$  and  $\theta_0$  are the minimum radius and braid angle, respectively.  $L_0$  is the maximum (initial) length, and  $\varepsilon$  is the contraction ratio. Equations (5) and (6) give a basis for predicting the generated muscle force. However, they fail to completely model the behaviour of braided muscle actuators due to the assumption of lossless operation. Subsequently, various hypotheses have been developed to account for the effects of tubing elasticity, internal frictions, braid thickness, stretching of the fibres, end cap diameter (i.e. non-cylindrical muscle shape) and material modeling in order to provide more accurate models [16, 17, 21–25]. Despite the improvements, errors between the predicted and measured force still exists. Especially in the case of Festo fluidic muscles, the models have been too inaccurate leading to a use of various corrective factors and exponential curve fitting methods [21, 25].

It has also been observed that there exists hysteresis in the muscles during operation caused mainly by friction present in the system. To account for the friction in the mathematical models, a constant force offset can be subtracted from or added into the calculated static force depending on whether the muscle is contracting or expanding [17]. In [21] a parameter  $k$  was introduced, which “tunes the slope of the considered static model” and matches the modeled data with the experimental values.

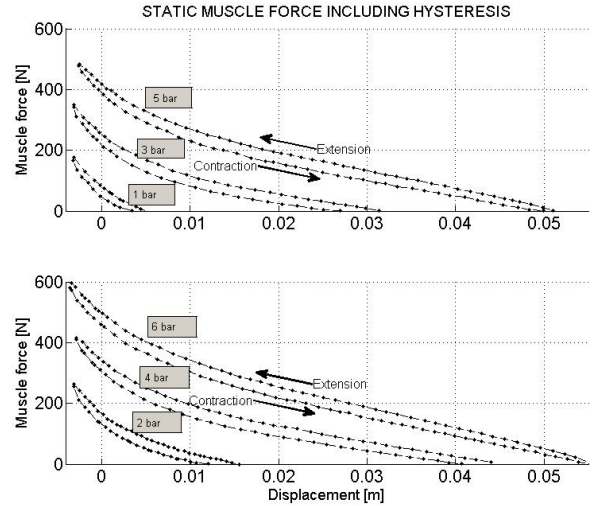


Fig. 3. Measured muscle force including hysteresis behavior

In Figure 3, the measured muscle force as a function of the displacement and pressure is shown, which also includes the hysteretic behavior of the Festo fluidic muscle. At the operating point  $x=0$ , the actuator is at rest and the positive displacement  $x$  refers to the amount of displacement/shortening of the actuator. The negative displacement indicates the stretching of the actuator from its nominal length. It should be noted that the actuator can provide even higher initial forces when pre-stretched. The force produced by the actuator decreases non-linearly as the contraction/displacement increases. When the actuator reaches its minimum length/maximum displacement the actuator does not provide any force.

The muscle actuator introduces a variable spring and a damper in parallel. The variable spring component is described by the static muscle force equation including hysteresis phenomena. The damper component describes the dynamics of the actuator including the viscous friction effect. For modeling the static force characteristics, averaged force/displacement curves at each pressure level are determined by calculating the average of the hysteresis loops shown in Figure 4. In order to capture the nonlinear force characteristics, an alternative fitting approach from the aforementioned methods is used. The maximum available force as a function of displacement is introduced by fitting a 4th-order polynomial function for the curve at the maximum pressure 0.6 MPa. As a result, the nonlinear curve shape of the force/displacement characteristics is captured. When the muscle displacement is held constant, the actuator force depends almost linearly on the pressure. However, the slope of the force per unit pressure changes as a function of the displacement and thus the muscle force can be described by:

$$F_{static} = F_{max}(x) - (p_{max} - p_m) \left( \frac{k_0 - k_1 x}{k_2} \right) \quad (7)$$

$$F_{max}(x) = a_0 + a_1 x + a_2 x^2 + a_3 x^3 + a_4 x^4$$

Where  $p_{max}$  is the maximum available muscle pressure and  $p_m$  is the current muscle pressure. Coefficients  $k_0$  [N],  $k_1$  [N/m], and  $k_2$  [Pa] are found by using least-squares methods.

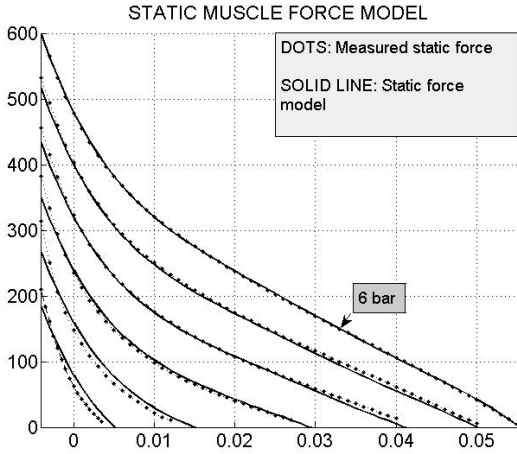


Fig. 4. Static muscle force model

Figure 4 illustrates the predicted force plotted against the measured force data at different pressure levels (0.1 to 0.6 MPa). The model is able to predict the force reasonably well for almost every pressure. Some deterioration exists between the model and actual data at lower pressure levels (less than 0.2 MPa).

For modeling the hysteresis, a similar approach as in [17] is used. The shape and the width of the hysteresis loops are almost the same for each pressure level as shown in Figure 3. An average value for the width of the hysteresis loop resulted in 32 N. Thus a friction force offset  $F_C$  (Coulomb friction) of 16 N can be added into the static force model described by the equation (7), as follows:

$$F_{muscle} = F_{max}(x) - (p_{max} - p_m) \left( \frac{k_0 - k_1 x}{k_2} \right) - F_C \text{sign} \left( \frac{dx}{dt} \right) \quad (8)$$

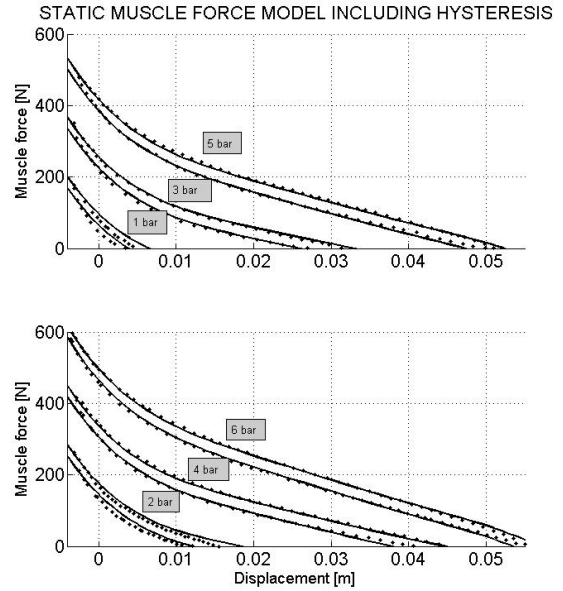


Fig. 5. Comparison between the modeled and actual force including hysteresis

In Figure 5, the muscle force model (equation (8)) is compared with the measured data. As a conclusion, the model is able to provide a reasonably good prediction for the muscle force, including the effect of hysteresis.

The identification of the viscous friction of the actuator is often a challenging task. The friction may be time-variant and dependent on the temperature and the pressure, as well as on the velocity. However, in our case, the effects of temperature and pressure are neglected. The goal here is to determine the viscous friction as a function of velocity with a reasonable amount of accuracy. In the analysis, a low-friction pneumatic cylinder is used in the measurement setup. First, the friction characteristics of the cylinder is determined, by driving it at different constant velocities and calculating the friction force with the help of the measured pressure in chambers of the piston side and piston rod side. When the cylinder piston is moving at a constant velocity, the differential force between the chambers can be assumed to be equal with the friction force. The friction characteristics of the combination of the muscle actuator and the cylinder can be measured directly by the load cell attached to the other end of the muscle actuator. The free end is connected to the cylinder piston. In the measurements, first the cylinder chamber is pressurized. Then at the given time step the chamber port is opened to ambient pressure and the muscle actuator is pressurized to create the motion. During this operation the displacement, force and cylinder pressure are measured which are then used to calculate the total friction force as a function of the velocity. A rough estimate of the viscous friction of the muscle actuator can be obtained by subtracting the cylinder friction from the total friction. Figure 6 shows the estimated friction of the cylinder, muscle actuator, and the combination of the two. Furthermore, it should be noted that the viscous friction is assumed to be symmetrical for positive and

negative velocities. A description of the total muscle force, which includes the behavior of friction, may be defined as follows:

$$F_{muscle} = F_{static} - F_c \text{sign}\left(\frac{dx}{dt}\right) - C_f \frac{dx}{dt} \quad (9)$$

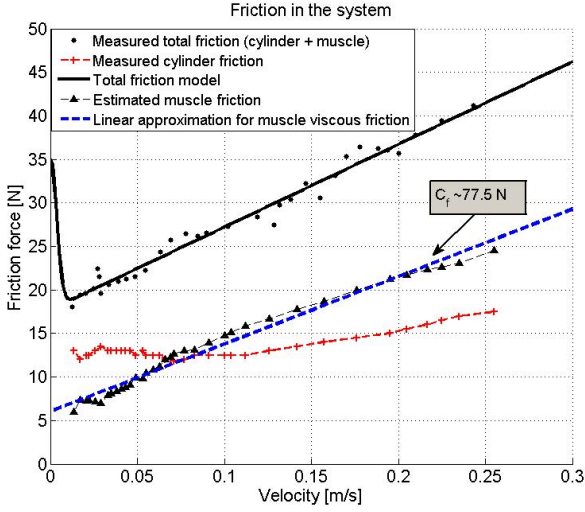


Fig. 6. Estimated friction characteristics of the muscle actuator

### Non-analytic valve model

The PWM pneumatic valve, that controls the airflow into and out of the actuator, is a fundamental component of the system. The valve considered in this study is a 3/2-high speed solenoid valve (Festo MHE2-1/8-MS1H-3/2G-M7) with a switching time of approximately 2 ms. The working principle of the solenoid valve is described as follows: the tensile force of the preloaded spring, and the force exerted by the air, tend to close the valve. Conversely, the magnetic force created by the current passing through the coils pushes the core and then the poppet, which opens the valve. The area of the air passage is a function of the position of the poppet, and it is also dependent on the diameter of the restricted passage, as well as the geometric form of the poppet. However, the internal structure of the solenoid valve is not usually known by the user and is not easily measured. Thus, it is not very efficient to establish a model that takes into account the electrical, magnetic, and mechanical subsystems of the component.

In general, the thermodynamics equations considered for valve modeling are those shown in literature for a gas through a nozzle, while assuming an adiabatic process, absence of losses, and convergent nozzle [26]. Thus, the mass flow rate passing through the valve can be expressed as follows:

$$\dot{m} = A p_{up} C_q C_m / \sqrt{T_{up}}$$

$C_q = \text{flow rate coefficient}$

$$C_m = \begin{cases} \sqrt{\frac{k}{R} \left(\frac{2}{k+1}\right)^{\frac{k+1}{k-1}}}, & \frac{p_{down}}{p_{up}} \leq p_{cr} \\ \sqrt{\frac{2k}{R(k-1)} \left[ \left(\frac{p_{down}}{p_{up}}\right)^{\frac{2}{k}} - \left(\frac{p_{down}}{p_{up}}\right)^{\frac{k+1}{k}} \right]}, & \frac{p_{down}}{p_{up}} \geq p_{cr} \end{cases} \quad (10)$$

Where  $T_{up}$  is the upstream air temperature and  $p_{up}$  is the upstream pressure,  $k=1.4$  is the specific heat ratio of air,  $p_{down}$  is the downstream pressure, and  $R=287$  J/kg/K is the air constant.  $C_q$  and  $C_m$  are, respectively, the flow rate coefficient and the flow rate parameter of the solenoid valve. The critical pressure  $p_{cr}$  divides the flow into sonic ( $p_{down}/p_{up} < p_{cr}$ ) and subsonic ( $p_{down}/p_{up} > p_{cr}$ ) flow regimes. The flow equation works well usually for a short convergent nozzle where the friction and compressibility effects are negligible. However, due to the flow rate losses in commercial valves, the critical pressure does not have a prefixed expression (usually 0.528) but it changes depending on the particular type of valve considered. As a result, we have found that the given flow rate equation does not correspond well to the mass flow rate characteristics of the solenoid valve under study.

Instead, a theoretical model introduced in [7, 27] is used. Here, the flow rate is considered constant in a sonic flow zone, while it decreases with a quadratic behavior approximated by a quarter of ellipse in the subsonic flow zone.

$$m = \begin{cases} C_v A \frac{p_{up}}{\sqrt{RT_{up}}} & \frac{p_{down}}{p_{up}} \leq b_v \\ C_v A \frac{p_{up}}{\sqrt{RT_{up}}} \sqrt{1 - \left[ \frac{\left(\frac{p_{down}}{p_{up}}\right) - b_v}{1 - b_v} \right]^2}, & \frac{p_{down}}{p_{up}} \geq b_v \end{cases} \quad (11)$$

$C_v$  is the valve discharge flow coefficient, and  $b_v$  is the critical pressure. In addition, the flow paths of the valve must be considered separately. In other words, the model should account for two possible flows. When the valve is open the flow path is through the orifice 1 - > 2 (inflation), and when the valve is closed the flow path is through the orifice 2-> 3 (deflation). While inflating, the upstream pressure is a constant supply pressure, and the downstream pressure is the pressure inside the actuator. When exhausting, the upstream pressure is the actuator pressure, and the downstream pressure is the ambient pressure.

In order to identify the pneumatic behavior of the valve a set of experiments according to the procedure introduced by ISO6358 were carried out. In measurements, three upstream pressure levels were used and the relevant experimental points were fitted by tuning two parameters ( $C_v$ ,  $b_v$ ) through equation (11). The geometric and tuned flow rate parameters are reported in Table 1. Figure 7 shows a good

overlap between the simulated and experimental curves. It should also be noticed that the valve's flow ways are not symmetrical.

Parameter	Description	Value
$R$	Air constant	287 [J/(kg*K)]
$T_{up}$	Upstream temperature	293 [K]
$p_{up}$	Upstream pressure	0.5,0.6,0.7 [MPa] (abs)
$A$	Valve diameter	3.14e-6 [m <sup>2</sup> ]
$C_v$ (1 -> 2)	Flow coefficient	0.36
$C_v$ (2 -> 3)	Flow coefficient	0.39
$b_v$ (1 -> 2)	Critical pressure	0.28
$b_v$ (2 -> 3)	Critical pressure	0.49

Table 1. Parameters used for valve identification

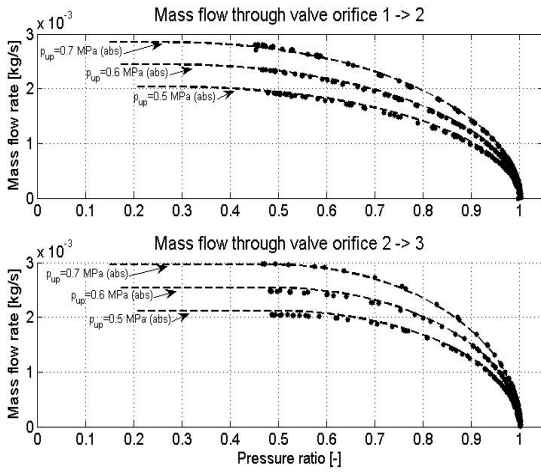


Fig. 7. Flow rate fits for passages 1->2 and 2->3

### Analytic valve model

It is quite obvious that the mass flow rate model of the 3/2 high speed on/off valve is an essential part of the system model. The solenoid valve is controlled with the duty ratio of the PWM-modulated signal. The time period of the PWM-signal is determined as  $T_{PWM}$  and is the inverse of the switching frequency  $T_{PWM} = 1/f_{PWM}$ . The switching time for opening and closing the valve is approximately 2 ms, which naturally reduces the maximum available duty cycle range. The switching frequency and the duty cycle determine how long the valve is open and closed during time period  $T_{PWM}$ . Valve delays and the discontinuous high frequency switching increase the complexity of the valve model, and are difficult to handle in the view point of controller design. Thus the non-analytic model introduced (equation (11)) is not feasible and an alternative valve model is needed. In a PWM-controlled system, the power is delivered to the actuator in discrete packets of fluid mass, as the valve is either completely open (on) or closed (off). If the switching frequency of the valve is significantly higher than the system dynamics, the system responds similarly as in the case of continuous mass flow. As the control signal for the valve is actually the duty

ratio, it is necessary to determine the average mass flow rate as a function of actuator pressure and duty ratio control signal.

In its place, a procedure similar to the one introduced in [28] is followed, where an equivalent mass flow rate model was determined for a proportional servo valve. The mass flow rate has nonlinear characteristics and is a function of pressure  $p$  inside the volume, and the control signal  $u$  (duty ratio [0-1]). Thus, one obtains a traditional representation for the pressure change as follows:

$$\dot{p} = \frac{kRT}{V} \dot{m}_{eq}(u, p) - kp \frac{\dot{V}}{V} \quad (12)$$

In equation (12), the second term can be computed once the volume  $V$  is known, and the pressure is given. In the first term, the nonlinear valve function is difficult to measure. Alternatively, the nonlinear valve characteristic can be approximated experimentally by charging and discharging a constant volume chamber. This causes the second term in equation (12) to disappear, allowing the mass flow rate to be calculated from the rate of change of pressure. A set of input signals with different duty cycles were applied to the valve and the pressure response in the constant volume chamber was measured. Due to the PWM switching, the pressure signal contains a significant amount of vibrations. Thus, the pressure response requires digital filtering in order to obtain an averaged response. The average pressure signal may then be differentiated in order to obtain the pressure change at different times. By distributing the computed slopes of the pressure curve at the corresponding parameter pairs ( $u$  and  $p$ ), a parametric representation of the surface of the pressure change can be obtained. Using this surface, the mass flow rate can be estimated using equation (12). Figure 8 illustrates the estimated/measured mass flow rate plotted as a function of input signal (duty ratio) and the relative actuator pressure. Note that a negative mass flow rate indicates a discharging flow.

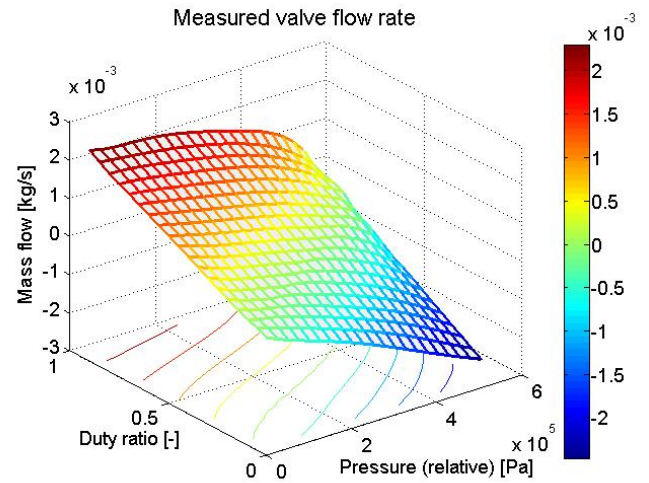


Fig. 8. Estimated mass flow rate for on/off valve

In order to model the mass flow rate, a 2<sup>nd</sup> order bi-polynomial function was used, as follows:

$$\begin{aligned} \dot{m}_{eq}(u, P_m) = & m_1 + m_2 P_m + m_3 P_m^2 + m_4 u + m_5 u P_m + m_6 u P_m^2 + m_7 u^2 \\ & + m_8 u^2 P_m + m_9 u^2 P_m^2 \end{aligned} \quad (13)$$

Where  $m_{1-9}$  are the coefficients found using the least-squares method.

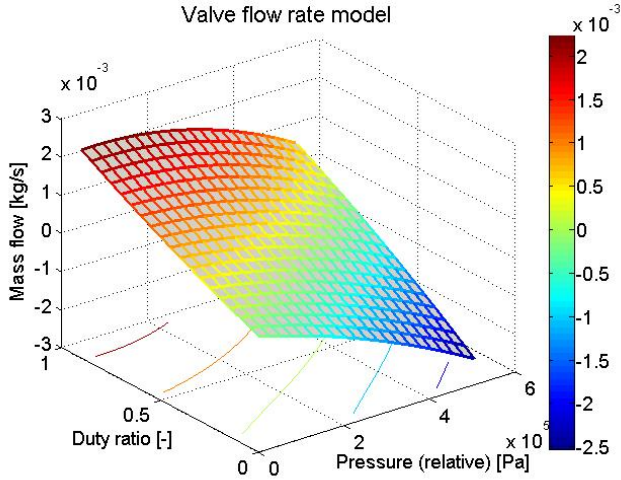


Fig. 9. Fitted model for mass flow rate

The output obtained from this function is plotted in Fig. 9. It can be observed that the model approximates the averaged mass flow rate behavior of the valve quite well. The maximum fitting error is  $1.96 \times 10^{-4}$  kg/s, or 4.13 % of the range. The RMSE is  $5.5 \times 10^{-5}$  kg/s or 1.16 %.

### Pressure dynamics

Knowledge of the actual pressure inside the muscle actuator is essential for understanding the dynamic behavior. The pressure depends on the mass of the air and the volume of the muscle. The diameter and length of the muscle were measured, and the volume of the muscle was calculated assuming a cylindrical shape. The volume shows a nearly linear behavior, dependent on displacement:

$$V_m(x) = v_0 + v_1 x, \quad (14)$$

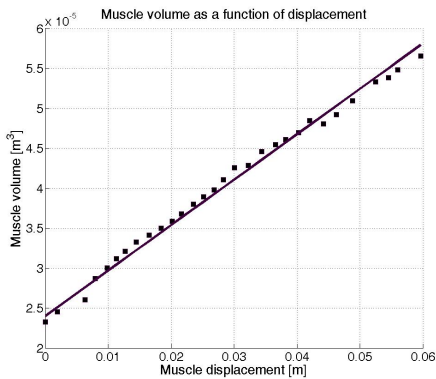


Fig. 10. Muscle volume in correlation with displacement

For calculating the pressure inside the muscle, it is assumed that the air is ideal gas and the change of air is adiabatic, such that the pressure change follows:

$$\dot{p}_m = \frac{kRT}{V_m(x)} \dot{m}_{eq}(u, p_m) - \frac{kp_m}{V_m(x)} \frac{dV_m(x)}{dx} \dot{x} \quad (15)$$

Where  $k$  (1.4 for adiabatic process),  $R$ ,  $T$ ,  $V_m$  and  $p_m$  denotes the specific heat ratio, gas constant, air temperature, volume of the muscle, and muscle pressure, respectively. The second main expression of equation (15) considers the power balance of the pressurized flow rate. The first term (following the subtraction sign) represents the pressure change due to the mass flow in or out of the muscle chamber. The second term represents the pressure change due to the change of the muscle chamber volume. The reciprocal volume takes into account the compressibility of the air.

### Overall system model

The motion equation of the muscle driving a constant payload attached in a vertical direction is defined (using Newton's Second Law) as follows:

$$M\ddot{x} = F_{static} - F_c \text{sign}\left(\frac{dx}{dt}\right) - C_f \frac{dx}{dt} - Mg \quad (16)$$

Where  $F_{static}$  is the static muscle force given in equation (7),  $M$  is the total mass of the system and payload, and  $g$  is the gravitational constant.  $F_c$  is the Coulomb friction, and  $C_f$  is an experimentally approximated damping factor of the muscle actuator.

In conventional analytical control approaches, such as sliding mode control, a state-space description of the system is preferred. Thus, suppose that the state vector for the system is defined as follows:

$$x_{states} = [P_m \quad x \quad \dot{x} \quad \ddot{x}]^T \quad (17)$$

From the nonlinear models described in the previous sections (particularly equations (7), (13), (15) and (16)), we have the following discrete-time equations which can be used in the control and estimation processes [31]:

$$x_{1,k+1} = \frac{kT_s}{v_0 + v_1 x_{2,k}} [RT \dot{m}_{eq}(u, x_{1,k}) - x_{1,k} v_1 x_{3,k}] + x_{1,k} \quad (18)$$

$$x_{2,k+1} = T_s x_{3,k+1} + x_{2,k} \quad (19)$$

$$x_{3,k+1} = \frac{T_s}{M} [F_{max}(x_{2,k}) - (P_{max} - x_{1,k}) \frac{k_0 - k_1 x_{2,k}}{k_2} - F_c \text{sign}(x_{3,k}) - C_f x_{3,k} - Mg] + x_{3,k} \quad (20)$$

$$x_{4,k+1} = \frac{x_{3,k+1} - x_{3,k}}{T_s} \quad (21)$$

It should be noted that the analytic mass flow rate model (equation (13)) enables the use of this kind of system presentation.

## SIMULATION AND EXPERIMENTAL RESULTS

This section describes the results of validating the developed valve models and overall system model with measurements. In addition, the final system model is used for tuning the parameters of a traditional PI-controller, which is used to control the actuator to follow a desired displacement trajectory.

### Valve model validation

In the previous section, two solenoid valve models were developed: non-analytical and analytical. The non-analytical valve model is based on equation (11) for which the tunable parameters were found by fitting the equation to match with experimental data. In the model, the flow paths of the valve are described separately, as the air flow is through passage 1->2 when the valve is “on” and through 2->3 when the valve is “off”. During the “on” state, the valve inflates the actuator volume, and the supply pressure is the upstream pressure while the actuator pressure is the downstream pressure. During the “off” stage, they are actuator pressure and ambient pressure, respectively. The non-analytical model also includes the valve delay (~2 ms) in the switching phenomena when the valve changes its state.

The measurements are carried out with a known constant volume. During the inflation process, the supply pressure is 5.5 Mpa (relative) and the initial pressure in the volume is zero. The volume is pressurized operating the solenoid valve with different duty ratios (25, 50 and 75 %) of 50 Hz PWM-signal. The chosen frequency is fast enough for the system dynamics and also provides a reasonable resolution for controlling the available duty ratio values. It should be noted, that the valve delay decreases the maximum available duty ratio range into 10-90% using this frequency. During the deflation process, the volume is first pressurized to a maximum value (5.5 MPa rel.), and then the valve is operated similarly with different duty ratios as in the inflation process.

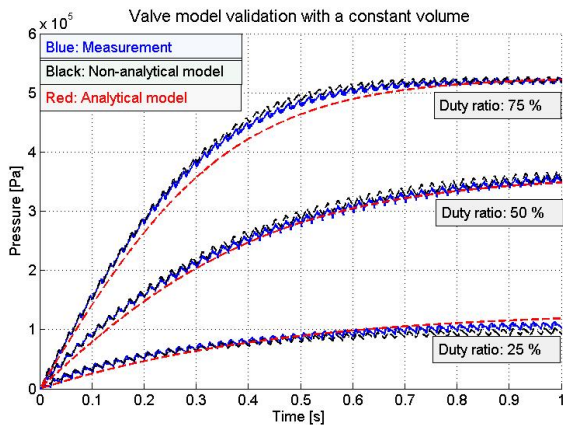


Fig. 11. The validation of valve models when inflating a constant volume with different PWM-duty ratios

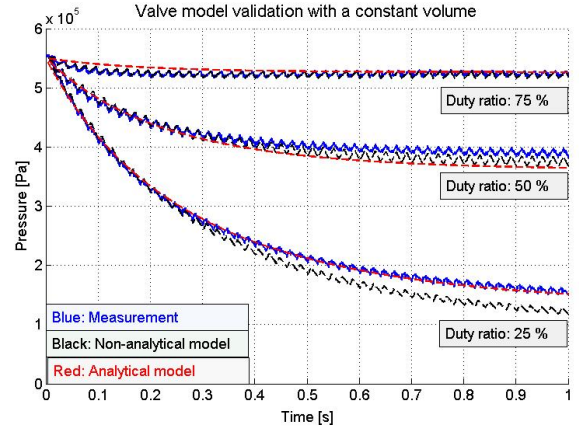


Fig. 12. The validation of valve models when deflating a constant volume with different PWM-duty ratios

Figures 11 and 12 illustrate the simulated and measured pressure responses for the inflation and deflation processes. The non-analytical valve model gives a good overall estimation for inflating pressure curves. However, the model is unable to completely estimate the pressure response during the deflation process. The deviation is caused by the silencer that was attached to the third valve port. The use of the silencer is necessary because of the very loud noise caused by the high speed valve switching. The silencer clearly changes the characteristics of the flow through 2 -> 3. The effects of the silencer on the pressure response are strongest when the pressure inside the volume approaches the steady-state value. As the pressure drop across the valve decreases the silencer slows down the flow. In consequence, the pressure in the simulations drops faster causing a steady-state offset compared to the measurements. The effects of the silencer at higher upstream pressure levels are almost negligible, and the model is able to follow the measured pressure curves quite accurately. Clearly, better estimation results would be gained if the valve was operated without the silencer.

The analytical valve model was described in the previous section. The purpose of it is to provide mass flow estimation through the valve as a function of the duty ratio and the pressure of the controlled volume. The model assumes that the supply pressure at the first valve port is constant (6.5 MPa abs.) and port 3 is at the ambient pressure. The valve relies heavily on the measurements that are naturally sensitive to the uncertainties. A large number of measurements were carried out and the pressure responses of the constant volume were measured. From the measured data, the pressure change was captured and the approximation for the average mass flow rate was calculated at different volumetric pressure levels and duty ratios. A 2<sup>nd</sup>-order bi-polynomial function was fitted to the obtained data with relatively good accuracy. The comparison of analytical model to the non-analytical model and measured pressure responses are shown in Figures 11 and 12, respectively. Despite some divergences between the model and the measurement, the model is able to estimate the pressure with reasonable accuracy. The advantage of the model is its suitability to be used for conventional control design, such as sliding mode control. The effectiveness of the model was proved in [29], where it was used successfully with the smooth variable structure filter (SVSF) to estimate the system states for the sliding mode controller. In the controller, a model based feed-forward control was used to provide an equivalent control signal

(duty ratio) for the valve. Based on the nonlinear state-space model (equations (18-21)), the equivalent desired mass flow may be estimated. The 2<sup>nd</sup>-order bi-polynomial function can then be solved to find the desired duty ratio when the desired flow rate and the actuator pressure (measured) are known. The sliding mode controller and the filter are known to be very robust to parameter variations and other uncertainties, yielding an error tolerance for the estimated mass flow rate model.

### System model validation

The overall model was verified for both the non-analytic and analytic valve models. In the validation process, a set of input signals (duty ratio) of triangle waveform was applied to the system. The frequency of the waveform was varied and the duty ratio value changed between 0.05 and 0.95. In the case of the non-analytical model, a pulse width modulator is used to convert the duty ratio signal into an appropriate on/off control ( $f=50$  Hz) for the valve.

The simulation and measurement results for input signal frequencies 0.08 and 0.25 Hz are shown in Figures 13 and 14. First of all, notice that the measured displacement signal contains no excessive chattering. The chosen PWM-frequency is thus high enough compared to the system dynamics. Although not shown here, the amplitude of chattering in the actuator pressure is approximately 15 kPa. An experiment with a PWM-frequency of 25 Hz resulted in an unacceptably large amount of chattering into the actuator displacement. An even smoother trajectory was gained with PWM-frequency of 100 Hz. The drawback of using that is the poor resolution of the input signal; even if an 0.1 ms sampling time is used.

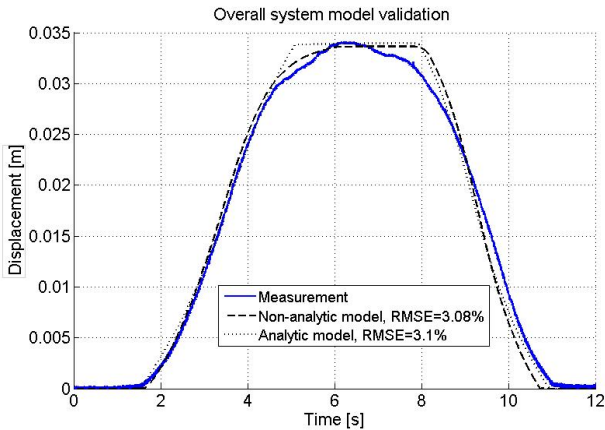


Fig. 13. Simulated and measured displacement response for a triangle ( $f=0.08$  Hz) input signal

The simulation results show that both models are able to estimate the displacement of the actuator and payload (9.6 kg) with reasonable good accuracy. An extremely good accuracy is obtained during the upward motion. The models fail to describe the creeping effect near the maximum displacement. It is a nominal effect for this type of actuator caused by material deformations. The largest modeling errors occur during the downwards motion. This is caused by the simplified hysteresis model where a constant force offset is either reduced from or added into the static muscle force model depending on the sign of the actuator velocity. Thus, the model does

not take into account the real transition between the inflating and deflating curves. As a result, the accuracy of the models is not as good compared to the upwards motion. In addition, the un-modeled silencer affects the accuracy of the non-analytical model. Altogether, both the models can estimate the real process reasonably well, as the maximum displacement error is approximately 10% and the RMSE values for the displacement are around 3-5%.

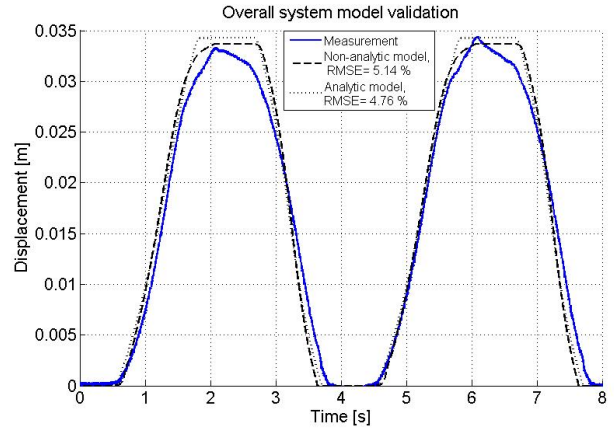


Fig. 14. Simulated and measured displacement response for a triangle ( $f=0.25$  Hz) input signal

### PI-Control

A PI-controller was tuned by trial-and-error using the non-analytical and analytical system models. During the operation it was noted that the system is very sensitive to oscillations and instability. The instability issue limited the maximum gains for the controller resulting in a lack of accuracy. A reasonable performance was gained with a derivative gain in the controller during the simulations, but due to the measurement noise it could not be used in the real system. Figures 15 and 16 illustrate the results when the input signal is sinusoidal with amplitude of 0.01 m and frequencies of 0.5 and 1 rad/s. The tuned gains for the controller were  $P=25$  and  $I=150$ . It can be seen that the system performance is quite poor with the PI-controller. The response for the initial step is slow, and the system is not able to follow the desired trajectory very well. A steady-state error of approximately 1.5-2.2 mm is present during the entire cycle. The RMSE is over 10%, and increases as the frequency of the desired trajectory is increased. It becomes apparent that pneumatic systems are very difficult to control accurately. The performance of traditional linear approaches like PI and PID controllers is poor with highly nonlinear pneumatic systems. Thus, nonlinear and robust approaches are needed for better performance. However, the models developed in this paper of the pneumatic muscle actuator system give a firm basis for the design of more advanced control strategies. The non-analytical model can be used to simulate the real process quite accurately. In addition, the analytical model can be used in the model-based controller and state estimator design.

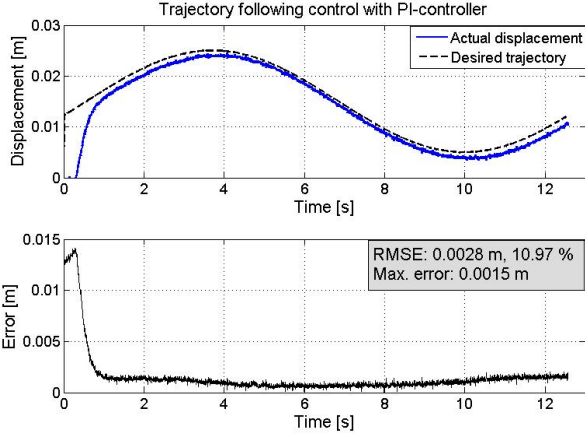


Fig. 15. Trajectory ( $\omega=0.5$  rad/s) followed control with tuned PI-controller

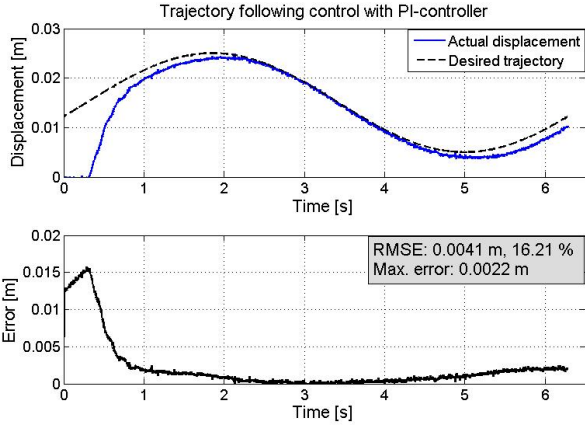


Fig. 16. Trajectory ( $\omega=1$  rad/s) followed control with tuned PI-controller

## CONCLUSIONS

In this paper, a nonlinear model for a pneumatic muscle actuator system controlled by an on/off solenoid valve was developed. The solenoid valve is operated by a pulse width modulated (PWM) scheme which gives an interesting alternative to develop low-cost pneumatic servo systems. On the other hand, accurate control of highly nonlinear pneumatic systems requires advanced control techniques that often use model-based approaches. Thus, the main focus of this research was to develop a model for control design approaches which capture the major nonlinearities present in the system with reasonable accuracy. In PWM-operated systems, the high speed switching of the valve results in discontinuities which are often difficult to handle from the viewpoint of control design. As a consequence, two valve models were developed in this study. The non-analytical model is able to describe the real operation of the system with relatively good accuracy, and including the nonlinear flow regimes and valve switching delays. The model is suitable for system analysis and for testing of controllers. The analytical model of the system, which includes the nonlinearities of the system, was developed to transform the discontinuities into a continuous form. This was accomplished by introducing a continuous flow model through the valve as a function of duty ratio of PWM-

signal and actuator pressure. The use of this analytical model enables the implementation of conventional analytical control approaches, such as sliding mode control, and provides a tool for the analysis of stability and robustness.

## NOMENCLATURE

$A$	[m <sup>2</sup> ]	effective orifice area of the valve
$C_f$	[Ns/m]	viscous friction coefficient
$C_m$	[-]	flow rate coefficient of the valve
$C_q$	[-]	flow rate parameter of the valve
$C_v$	[-]	discharge flow coefficient of the valve
$D, D_0$	[m]	muscle actuator diameter
$F$	[N]	force in general
$F_c$	[N]	Coulomb friction
$F_{max}$	[N]	maximum muscle force muscle
$F_{muscle}$	[N]	force generated by the muscle
$L, L_0$	[m]	muscle length, initial length
$M$	[kg]	weight of the payload (9.6 kg)
$p_{cr}$	[Pa]	critical pressure ratio
$p_{down}$	[Pa]	downstream pressure
$p_m$	[Pa]	pressure inside the muscle
$p_{up}$	[Pa]	upstream pressure
$p_s$	[Pa]	supply pressure
$p_0$	[Pa]	atmosphere pressure
$R$	[J/(kgK)]	gas constant
$T$	[K]	air temperature
$T_{up}$	[K]	upstream air temperature
$T_{PWM}$	[s]	time period of PWM-signal
$T_S$	[s]	sampling time
$V$	[m <sup>3</sup> ]	volume in general
$V_m$	[m <sup>3</sup> ]	volume of the muscle
$a_{0-4}$	[m]	muscle force coefficients
$b_s$	[m]	length of one braid strand
$b_v$	[m]	critical pressure
$f_{PWM}$	[Hz]	switching frequency of the PWM-signal
$g$	[m/s <sup>2</sup> ]	gravity constant
$k$	[-]	specific air heat ratio
$k_0$	[N]	coefficient for muscle force eq.
$k_1$	[N/m]	coefficient for muscle force eq.
$k_2$	[Pa]	coefficient for muscle force eq.
$\dot{m}_{eq}$	[kg/s]	equivalent mass flow rate
$\dot{m}$	[kg/s]	mass flow rate
$m_{1-9}$	[-]	coefficients for eq. mass flow rate
$n_s$	[-]	number of strand encircles
$p$	[Pa]	pressure
$p_{cr}$	[Pa]	critical pressure ratio
$p_{down}$	[Pa]	valve downstream pressure
$p_m$	[Pa]	pressure inside the muscle
$p_{max}$	[Pa]	maximum muscle pressure
$p_0$	[Pa]	atmosphere pressure
$p_u$	[Pa]	valve downstream pressure
$r_0$	[m]	initial muscle radius
$u$	[-]	control signal (duty ratio)
$u_{eq}$	[-]	equivalent control signal
$x$	[m]	displacement of the muscle
$\theta, \theta_0$	[°]	muscle braid angle, initial braid angle
$\varepsilon$	[-]	muscle contraction ratio
$v_0, v_l$	[m <sup>3</sup> , m <sup>2</sup> ]	muscle volume coefficient
$\cdot$	[-]	denotes a time derivative

## REFERENCES

- [1] Morita, Y.S., Shimizu, M., and Kagawa, T., An Analysis of Pneumatic PWM and its Application to a Manipulator, Proc. of International Symposium of FluidControl and Measurement, Tokyo, pp. 3–8, 1985.
- [2] Noritsugu, T., 1986, Development of PWM Mode Electro-Pneumatic Servomechanism, Part I: Speed Control of a Pneumatic Cylinder, *J. Fluid Control*, 17–1, pp. 65–80.
- [3] Noritsugu, T., 1986, Development of PWM Mode Electro-Pneumatic Servomechanism, Part II: Position Control of a Pneumatic Cylinder, *J. Fluid Control*, 17–2–, pp. 7–31.
- [4] Lai, J.-Y., Singh, R., and Menq, C.-H., Development of PWM Mode Position Control for a Pneumatic Servo System, *Journal of the Chinese Society of Mechanical Engineers*, Vol. 13, No. 1, pp. 86–95, 1992.
- [5] Kunt, C., and Singh, R., 1990, A Linear Time Varying Model for On-Off Valve Controlled Pneumatic Actuators, *ASME J. Dyn. Syst., Meas., Control*, 112–4, pp. 740–747.
- [6] Ye, N., Scavarda, S., Betemps, M., and Jutard, A., 1992, Models of a PneumaticPWM Solenoid Valve for Engineering Applications, *ASME J. Dyn.Syst., Meas., Control*, 114–4, pp. 680–688.
- [7] Messina, A., Giannoccaro, N.I., and Gentile, A., Experimenting and modeling the dynamics of pneumatic actuators controlled by pulse width modulated technique, *Mechatronics*, No. 15, pp. 859–881, 2005.
- [8] Barth, E., Zhang, J., Goldfarb, M., Sliding mode approach to PWM-controlled pneumatic systems, *Proceedings of the American Control Conference*, pp. 2362-2367, Anchorage, AK, 2002
- [9] Ning, S., Bone, G., Development of a nonlinear dynamic model for a servo pneumatic positioning system, *Proceedings of the IEEE International Conference on Mechatronics and Automation*, pp. 43-48, Niagara Falls, Canada, 2005
- [10] Paul, A. K., Mishra, J. K., and Radke, M. G., 1994, Reduced Order Sliding Mode Control for Pneumatic Actuator, *IEEE Trans. Control Syst. Technol.*, 2–30, pp. 271–276.
- [11] Van Varseveld, R. B., and Bone, G. M., 1997, Accurate Position Control of a Pneumatic Actuator Using On/Off Solenoid Valves, *IEEE/ASME Trans. Mechatron.*, 2–30, pp. 195–204
- [12] Barth, E. J., Zhang, J., and Goldfarb, M., 2003, Control Design for Relative Stability in a PWM-Controlled Pneumatic System, *ASME J. Dyn. Syst., Meas., Control*, 125–3, pp. 504–508.
- [13] Shen, X., Zhang, J., Barth, E., and Goldfarb, M., Nonlinear averaging applied to the control of pulse width modulated (PWM) pneumatic systems, *Proceedings of the American control Conference*, pp. 4444–4448, Boston, 2004.
- [14] Shen, X., Zhang, J., Barth, E., and Goldfarb, M., Nonlinear Model-Based Control of Pulse Width Modulated Pneumatic Servo Systems, *Journal of Dynamic Systems, Measurement and Control*, September 2006, Vol. 128, pp. 663–669.
- [15] Taghizadeh, M., Ghaffari, A., and Najafi, F., A Linearization Approach in Control of PWM-Driven Servo-Pneumatic Systems, 40<sup>th</sup> Southeastern Symposium on Systems Theory (SSST), March 2008, pp. 395–399.
- [16] Schulte, R.A., The characteristics of the McKibben artificial muscle, In the Applications of External Power in Prosthetics and Orthotics. Publ. 874, Nas-RC, pp. 94–115, 1962.
- [17] Chou, P., and Hannaford, B., Measurement and Modeling of a McKibben Pneumatic Artificial Muscles, *IEEE Transactions on Robotics and Automation*, Vol. 12, No. 1, Feb 1996.
- [18] Festo, Fluidic Muscle MAS, Festo Brochure, 2002
- [19] Gaylord, R. H., Fluid Actuated Motor System and Stroking Device, US Patent No. 2,844,126. July 22, 1958.
- [20] Inoue, K., Rubbertuators and applications for robotics, In 4th International Symposium on Robotics Research, pp. 57–63, 1987.
- [21] Tondou, B., and Lopez, P., Modeling and Control of McKibben Artificial Muscle, *IEEE Control Systems Magazine*, pp. 15–38, April 2000.
- [22] Klute, G. K., and Hannaford, B., Accounting for elastic energy storage in McKibben artificial muscle actuators, *ASME Journal of Dynamic Systems, Measurement and Control*, Vol. 122, 2000.
- [23] Delson, N., Hanak, T., Loewke, K., and Miller, D.N., Modeling and implementation of McKibben Actuators for a Hopping Robot.
- [24] Davis, S., and Caldwell, D. G., Braid effects on contractile range and friction modeling in pneumatic muscle actuators, *The International Journal of Robotics Research*, Vol. 25, No. 4, April 2006, pp. 359–369.
- [25] Kerscher, T., Albiez, J., Zöllner, J. M., and Dillman, R., FLUMUT – Dynamic Modelling of Fluidic Muscles Using Quick-Releases, *Proceedings of the 3<sup>rd</sup> International Symposium on Adaptive Motion in Animals and Machines*, Illmenau, Germany, 2005
- [26] Shearer, J.L., Study of pneumatic processes in the continuous control of motion with compressed air (I, II), *ASME Trans.*, pp.233–249, 1956.
- [27] ISO6358, Pneumatic Fluid Power – Components using Compressible Fluids – Determination of Flow-rate Characteristics, 1989
- [28] Rao, Z., and Bone, G. M., Nonlinear modeling and control of servo pneumatic actuators, *IEEE Transactions on Control Systems Technology*, Vol. 16, No. 3, pp. 562–569, May 2008.
- [29] Jouppila, V., Gadsden, A., Habibi, S., Bone, G. M., Ellman, A., Sliding mode controller and filter applied to a pneumatic McKibben muscle actuator, In *ASME International Mechanical Engineering Congress and Exposition (IMECE2009)*, 10 pages, Lake Buena Vista, USA 2009